



INTERACTION OF GLUTATHIONE (REDUCED) WITH $[(H_2O)(TAP)_2RuORu(TAP)_2(H_2O)]^{2+}$ (TAP = {2-(M-TOLYLATO)PYRIDINE}) ION AT PHYSIOLOGICAL PH IN AQUEOUS MEDIUM.

TANDRA DAS(KARFA)^A, SUBALA MONDAL^A, ASOK K DATTA^B, BIPLAP K BERA^A, PARNAJYOTI KARMAKAR^A, SUBHASIS MALLICK^A, ARUP MANDAL^A AND ALAK. K GHOSH^{A*}

^ADepartment of Chemistry, The University of Burdwan, Burdwan-713104, West Bengal, India

^BBankura Sammilani Medical College, Bankura-722102, West Bengal, India

ABSTRACT

Kinetic and mechanistic studies on the interaction of glutathione (reduced) with the title complex at physiological pH and in aqueous medium have been done spectrophotometrically as a function of $[(H_2O)(tap)_2RuORu(tap)_2(H_2O)]^{2+}$, [glutathione], pH and temperature at constant ionic strength. The interaction reaction followed two parallel paths: both the paths are dependent on [ligand] and showed a limiting nature at higher concentration of the ligand. Rate constants ($k_1 \sim 10^{-3} \text{ s}^{-1}$, $k_2 \sim 10^{-5} \text{ s}^{-1}$), activation parameters and thermodynamic parameters (ΔH_1° , ΔS_1°) were calculated. A rate law involving the outer sphere association complex formation has been established at pH 7.4 for path 1 as

$$\text{Rate} = k_1 K_E [\{ (H_2O)(tap)_2RuORu(tap)_2(H_2O) \}^{2+}] [\text{ligand}] / (1 + K_E [\text{ligand}])$$

A mechanism involving the prior formation of an outer sphere complex followed by associative interchange (I_a) is proposed for both the paths where bond making and bond breaking are equally important in the transition state. Negative ΔG° values at all temperatures studied, also supports this proposition. IR and ESI-MS studies all help to propose the plausible mechanism.

Keywords: Ruthenium(II) . Glutathione . Interaction . Physiological pH . Aqueous medium

INTRODUCTION

The successful development of metal-containing anticancer drugs starts with the serendipitous discovery of *cis*-dichlorodiammineplatinum(II) or commonly called *cis*-platin as an anticancer drug [1-4]. Studies in this area are mainly limited to structural identification using NMR, ESI-MS and X-ray crystallographic techniques [2]. A negligible amount of work has been done in the reactivity, i.e., kinetic and mechanistic understanding of how metal complexes achieve their activities is crucial in

rationalizing the efficiency of the metallo-drugs in biological conditions.

Many potential alternative metallopharmaceuticals have been developed, based on platinum or other transition metals with ruthenium being one of the most promising [5,6].

Different studies reveal that a number of ruthenium compounds serve as bacterial mutagens and are capable of damaging genetic material [7-11].

It is observed that being a 4d congenor of iron, the most important biological metal in the periodic table, ruthenium complexes are less toxic [12,13].

Furthermore it is observed that in case of chloro-complexes the toxicity arises mainly due to the hydrolysis side products. If we use an aqua variety, the toxicity is reduced as well as the reaction becomes more straightway, i.e. an aqua variety is superior to others [14].

Another point of interest is that DNA is not the only target. Binding to protein and RNA also occurs as has been shown [15-18] by many investigators.

In continuation of studying [19] the reactivity of ruthenium (II) complex with different amino acid constituents, peptides, nucleosides, nucleotides and other bioactive ligands, in the present article we have discussed the mechanistic aspects of interaction of glutathione, an important tri peptide with the title complex in aqueous medium, where ruthenium(II) is stable even at biological condition (pH 7.4) due to the presence of strong pi-acceptor ligand tap (tap = {2-(m-tolylazo)pyridine}) [20]

Glutathione [21-24] is a ubiquitous tripeptide (γ -L-Glu-L-Cys-Gly) molecule, the predominant nonprotein thiol, consisting of three amino acids joined together. These are cysteine, glutamic acid and glycine-three of the twenty two amino acids

which comprise the building blocks of all known proteins.

We hope such a study will enrich the bioinorganic chemistry of ruthenium(II) and hence its application towards biological systems.

MATERIALS AND METHODS

Reported method, as discussed earlier [19] was used to isolate *cis*-diaqua-bis-{2-(m-tolylazo)pyridine} ruthenium(II) perchlorate, monohydrate, *cis*-[Ru(tap)₂(H₂O)₂](ClO₄)₂.H₂O and the compound was characterised by elemental analyses and spectral data ($\lambda_{\text{max}} = 536$ nm). The reacting complex ion [(H₂O)₂RuORu(tap)₂ (H₂O)]²⁺ (**1**) was generated *in situ* by adjusting the pH at 7.4. The reaction product $[(\text{tap})_2\text{Ru}(\mu\text{-O})(\mu\text{-GSH})\text{Ru}(\text{tap})_2]^{2+}$ (**Complex 2**) of glutathione and complex **1** was prepared by mixing them in different proportions *viz.* 1:1, 1:2, 1:3, 1:5 and 1:10 and thermostated at 60°C for 72h. The absorption spectra exhibited almost same absorbance in all cases. The difference in spectrum between complex **1** and complex **2** is shown in Figure 1. The electronic spectrum of **2** (Figure 1) shows excellent complexation

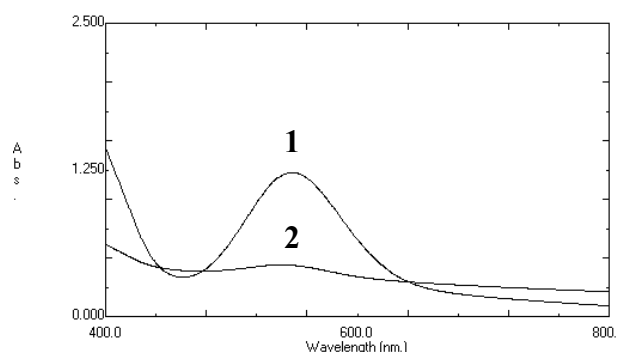
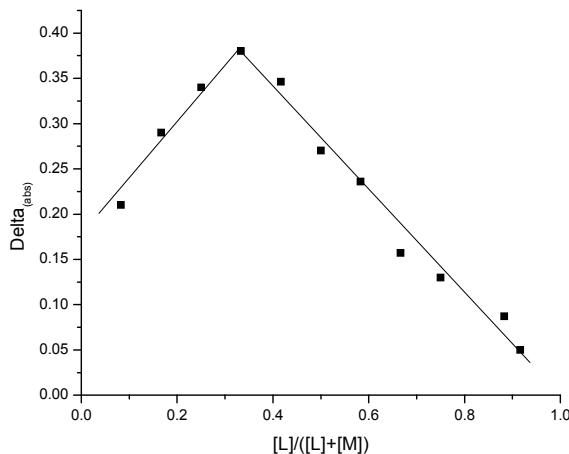


Figure 1. Difference in spectrum between Complex 1 and product complex (2). $[1] = 1.0 \times 10^{-4} \text{ mol dm}^{-3}$, $[GSH] = 2.0 \times 10^{-3} \text{ mol dm}^{-3}$, cell used 1 cm quartz.

between glutathione (reduced) and **1**. The composition of **2** in solution was determined by the Job's method of continuous variation and the metal : ligand ratio was found to be 2:1 (Figure 2).

**Figure 2. Job's Plot**

The pH of the solution was adjusted by adding NaOH/HClO₄ and the measurements were carried out with the help of a Sartorius make digital pH meter (PB 11) with an accuracy of ± 0.01 unit. Doubly distilled water was used to prepare all the kinetic solutions. All chemicals used were of AR grade available commercially. The reactions were carried out at constant ionic strength (0.1 M NaClO₄).

Kinetics Kinetic measurements were carried out on a Shimadzu UV 2101 PC spectrophotometer attached to a thermoelectric cell temperature controller (model TB 85 thermo bath, accuracy $\pm 0.1^\circ$). The conventional mixing technique was followed and

pseudo-first order conditions were employed throughout. The progress of the reaction was followed by measuring the decrease in absorbance at 560 nm, where the difference in absorbance between the substrate and the product complex is maximum. Plots of $\ln(A_t - A_\infty)$ against time, where A_t and A_∞ are the absorbance at time t and at infinite time (or after the completion of the reaction) are non-linear, it is curved at the initial stage and subsequently of constant slope (Figure 3). The method of Wyeh and Hamm [25] was adopted to calculate the rate constants for two

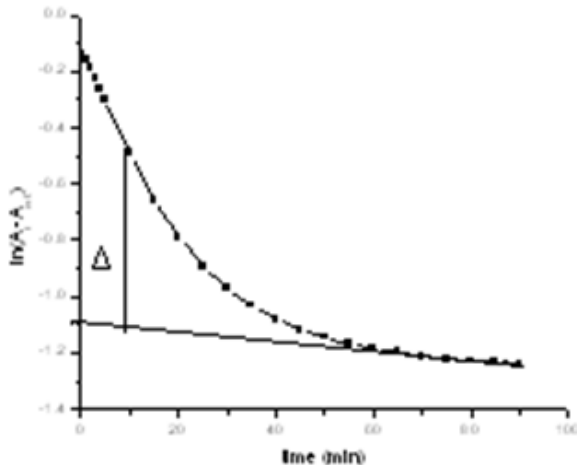


Figure 3. A typical plot of $\ln(A_t - A_\infty)$ versus time
 $[I] = 1.0 \times 10^{-4} \text{ mol dm}^{-3}$, $[GSH] = 2.0 \times 10^{-3} \text{ mol dm}^{-3}$, cell used = 1 cm quartz,
 $pH = 7.4$, medium = aqueous, temp. = 45°C

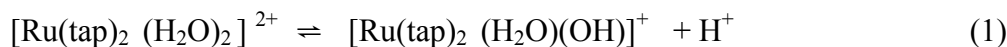
consecutive steps. From linear second portion $k_{2(\text{obs})}$ values were obtained. The $k_{1(\text{obs})}$ values were obtained from the plot of $\ln \Delta$ (the meaning of Δ is shown in Figure 3) versus t . A typical plot is shown in Figure 4. The rate data represented as an average of duplicate runs are reproducible within $\pm 4\%$.

Results and discussion

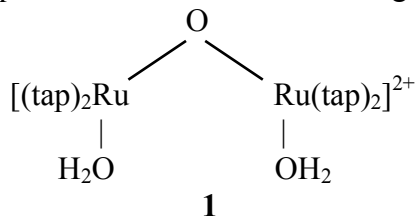
The first acid dissociation equilibrium of the complex

$[\text{Ru}(\text{tap})_2(\text{H}_2\text{O})_2]^{2+}$ is 6.6 [26] at 25°C.

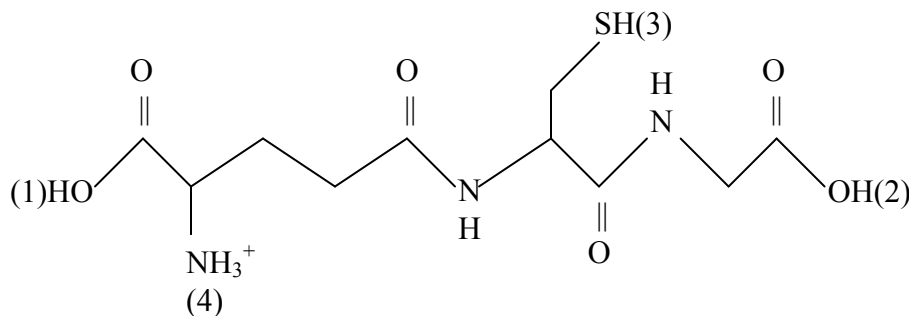
K_a



At pH 7.4 the complex exists in dimeric oxo-bridged form, $[(\text{H}_2\text{O})(\text{tap})_2\text{RuORu}(\text{tap})_2(\text{H}_2\text{O})]^{2+}$ [27-30].



The pK_1 , pK_2 , pK_3 and pK_4 values [31,32] of glutathione (GSH) are 2.05, 3.4, 8.72 and 9.49 respectively at 25°C. The fully protonated form of the ligand is



The equilibria are:



The Job's method of complexation indicates a 2:1 metal-ligand ratio in the product complex. It is possible only when a bridged product is formed with glutathione. At constant temperature, pH(7.4) and fixed concentration of complex 1 the $\ln(\text{A}_t - \text{A}_\infty)$ versus time (t) plots for different ligand concentrations indicate a two step process, both of which are dependent on incoming ligand concentration, and with increasing ligand concentration a

limiting rate is reached. The rate constant for such process can be evaluated by assuming the following scheme 1:



Scheme 1. Progress of the reaction in two parallel paths

Calculation of k_1 value

The rate constant $k_{1(\text{obs})}$ for the first path was evaluated by the method of Weyh and Hamm [25] using usual consecutive rate law:

$$(A_t - A_\infty) = a_1 \exp(-k_{1(\text{obs})}t) + a_2 \exp(-k_{2(\text{obs})}t) \quad (3)$$

$$\text{Or, } (A_t - A_\infty) - a_2 \exp(-k_{2(\text{obs})}t) = a_1 \exp(-k_{1(\text{obs})}t) \quad (4)$$

where a_1 and a_2 are constants dependent upon rate constants and extinction coefficient. Values of $[(A_t - A_\infty) - a_2 \exp(-k_{2(\text{obs})}t)]$ are obtained from X-Y at different time t (Figure 3) so that

$$\Delta = a_1 \exp(-k_{1(\text{obs})}t)$$

$$\text{or, } \ln \Delta = \text{constant} - k_{1(\text{obs})}t \quad (5)$$

$k_{1(\text{obs})}$ is derived from the slope of $\ln \Delta$ versus time, when t is small (Figure 4).

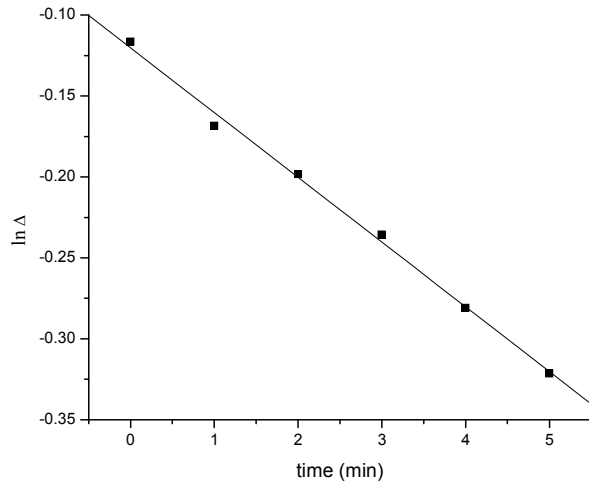


Figure 4. A typical plot of $\ln \Delta$ versus time

$[1] = 1.0 \times 10^{-4} \text{ mol dm}^{-3}$, $[\text{GSH}] = 2.0 \times 10^{-3} \text{ mol dm}^{-3}$, cell used = 1 cm quartz, pH = 7.4, medium = aqueous, temp. = 45°C

A similar procedure is applied for each ligand concentration in the $1.0 \times 10^{-3} \text{ mol dm}^{-3}$ to $5.0 \times 10^{-3} \text{ mol dm}^{-3}$ range at constant complex 1 concentration of $1.0 \times 10^{-4} \text{ mol dm}^{-3}$ at pH 7.4 in the 35° – 50°C temperature range and at constant ionic strength (0.1 mol dm^{-3} NaClO_4). The $k_{1(\text{obs})}$ values are collected in Table 1. The rate increases with increase in [Ligand] and reaches a limiting value (Figure 5).

Table 1. $10^3 k_{1(obs)}$ values for different ligand concentrations at different temperatures. [Complex] = 1×10^{-4} mol dm⁻³, pH = 7.4, ionic strength = 0.1 mol dm⁻³ NaClO₄.

10^3 [Ligand] (mol dm ⁻³)	Temperature (°C)			
	35	40	45	50
2.0	1.08	1.23	1.54	1.87
2.5	1.21	1.49	1.91	2.55
3.0	1.45	1.72	2.21	2.65
4.0	1.82	2.22	2.68	3.23
5.0	2.12	2.3	2.89	3.45

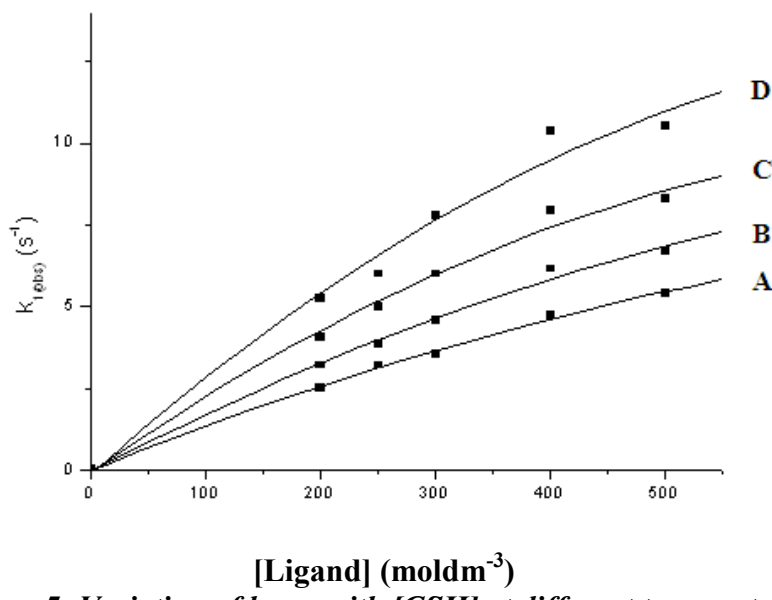
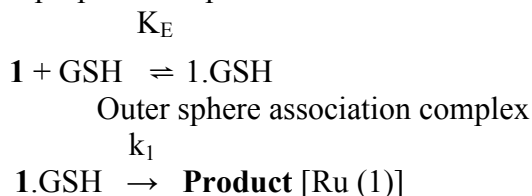


Figure 5. Variation of $k_{1(obs)}$ with [GSH] at different temperatures, A = 45, B = 50, C = 55 and D = 60°C

The limiting rate is probably due to the completion of outer sphere association complex formation. Since the metal ion reacts with immediate environment, further change in [Ligand] beyond the saturation point will not affect the reaction rate and a gradual approach towards limiting rate was observed. The outer sphere association complex is possibly stabilised through H-bonding [33,34]. Based on the experimental findings, the following Scheme 2 may be proposed for path 1:



Scheme 2. Proposed reaction pathway for path 1.

Based on the above scheme a rate expression can be derived for path 1

$$d[\text{Product}]/dt = k_1 K_E [\{(\text{H}_2\text{O})(\text{tap})_2\text{RuORu}(\text{tap})_2(\text{H}_2\text{O})\}^{2+}][\text{GSH}] / (1 + K_E[\text{GSH}]) \quad (6)$$

$$\text{or, } d[\text{Product}]/dt = k_{1(obs)} [\{(\text{H}_2\text{O})(\text{tap})_2\text{RuORu}(\text{tap})_2(\text{H}_2\text{O})\}^{2+}]_T \quad (7)$$

T stands for total concentration of Ru(II)

$$\text{We can write, } k_{1(obs)} = k_1 K_E [\text{GSH}] / (1 + K_E[\text{GSH}]) \quad (8)$$

where k_1 is the anation rate constant for step 1, i.e., the anation rate constant for the interchange of outer sphere complex to the inner sphere complex; K_E is the outer sphere association equilibrium constant.

This equation can be represented as

$$1/k_{1(\text{obs})} = 1/k_1 + 1/k_1 K_E [GSH] \quad (9)$$

The plot of $1/k_{1(\text{obs})}$ against $1/[GSH]$ is linear (Figure 6) with an intercept of $1/k_1$ and slope $1/k_1 K_E$.

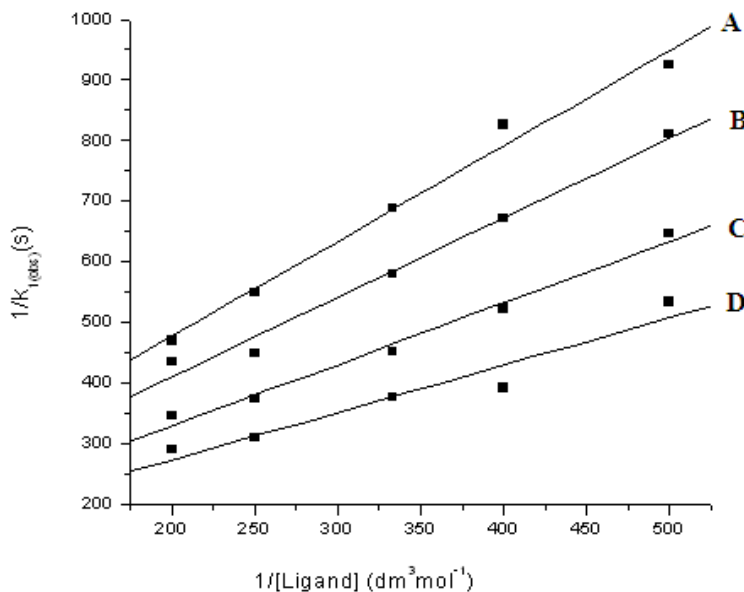


Figure 6. Plot of $1/k_{1(\text{obs})}$ versus $1/[GSH]$ at different temperatures, A = 45, B = 50, C = 55, and D = 60° C

This was found to be so at all temperatures studied. The k_1 and K_E values obtained from the intercept and from slope to intercept ratios are given in Table 3.

Calculation of k_2 value

The rate constants for path 2 were calculated from latter linear portions of the graphs and are collected in Table 2. This is again dependent on [Ligand] and shows a limiting value at higher concentration of the ligand (Figure 7).

Table 2. $10^5 k_{2(\text{obs})}$ values for different ligand concentrations at different temperatures. [Complex] = 1×10^{-4} mol dm $^{-3}$, pH = 7.4, ionic strength = 0.1 mol dm $^{-3}$ NaClO $_4$.

10^3 [Ligand] (mol dm $^{-3}$)	35	40	45	50
2.0	2.49	3.21	4.08	5.2
2.5	3.2	3.85	5.0	6.0
3.0	3.55	4.6	6.0	7.8
4.0	4.73	6.15	7.93	10.4
5.0	5.4	6.71	8.33	11.44

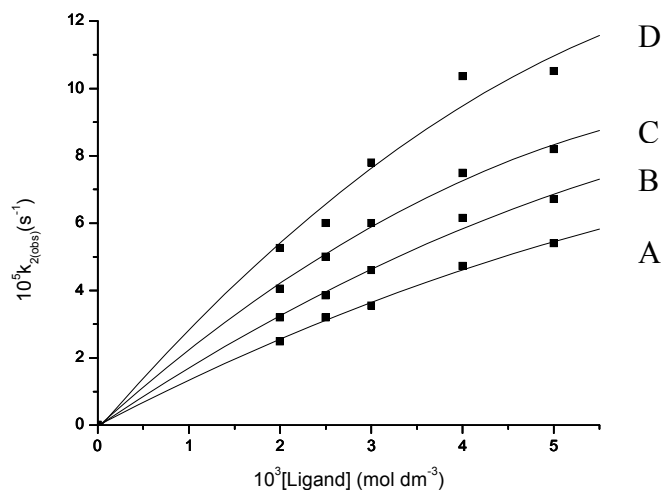


**Figure 7. Variation of $k_{2(obs)}$ with $[GSH]$ at different temperatures,
A = 45, B = 50, C = 55, and D = 60° C**

The intermediate here also possibly stable through H-bonding between coordinated water and the approaching glutathione. The value of k_2 and K_E' for path 2 were calculated by similar analysis to equation (9) (Figure 8) and collected in Table 3.

Table 3. The k_1 , K_E , k_2 and K_E' values for the interaction of glutathione with (1)

Temp. (°C)	$10^3 k_1$ (s ⁻¹)	K_E (dm ³ mol ⁻¹)	$10^5 k_2$ (s ⁻¹)	K_E' (dm ³ mol ⁻¹)
35	6.12	104	27.57	50
40	6.70	113	33.78	52
45	7.70	130	39.87	57
50	8.49	151	49.85	60

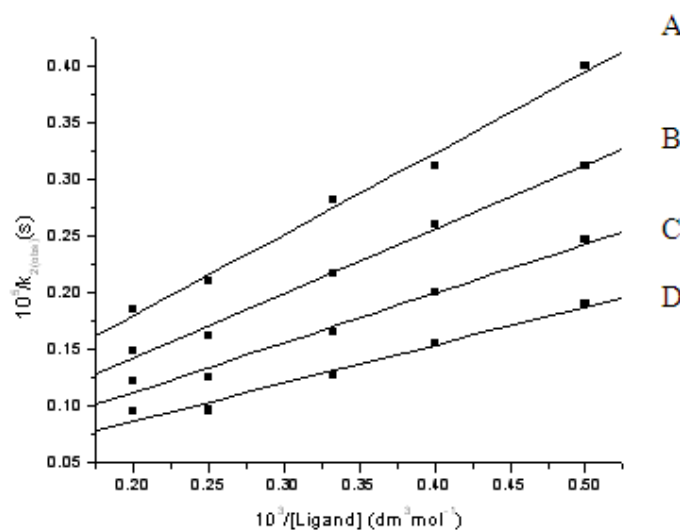


**Figure 8. Plot of $1/k_{2(obs)}$ against $1/[GSH]$ at different temperatures,
A = 45, B = 50, C = 55, and D = 60°**

IR study also substantiates the proposed mechanism. $[(\text{H}_2\text{O})_2(\text{tap})_2\text{RuORu}(\text{tap})_2(\text{H}_2\text{O})^{2+}]$ and glutathione were mixed in 2:1 molar ratio at pH 7.4 and a light-violet product was obtained. The IR spectra of the light-violet compound in the KBr disc shows strong bands at 3407 and 1642 cm^{-1} together with prominent bands at 1122, 688 and 475 cm^{-1} . The asymmetric COO^- stretching frequency (vasym) of the amino acids occurs at 1580–1660 cm^{-1} when the group is coordinated to metals, whereas a noncoordinated COO^- group has the vasym (COO^-) stretching at lower frequencies [35]. The band at

1642 cm^{-1} is therefore due to the vasym (COO^-) of the metal bounded carboxyl group. The presence of a strong stretching band at 3407 cm^{-1} indicates that the product is hydrated. The presence of weak absorption of –SH group at *ca.* 2500 cm^{-1} , present in free glutathione, indicates that the –SH group do not participate in bonding [36]. The bands at 688 and 476 cm^{-1} are also assigned as $\nu(\text{Ru}-\text{O})$ and $\nu(\text{Ru}-\text{N})$ bond formation respectively [37]. The IR spectrum suggests that the final product is an (O, N) coordinated chelate and glutathione behaves like a bidentate ligand in the experimental pH.

ESI-MS analysis (Fig. 9) shows a characteristic peak of the 2:1 metal-ligand coordination.

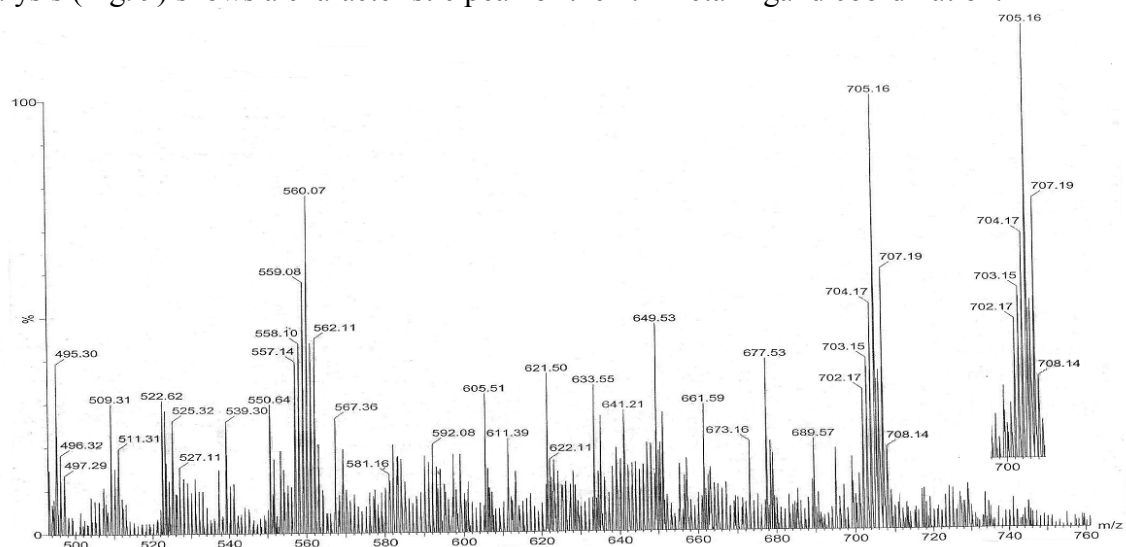
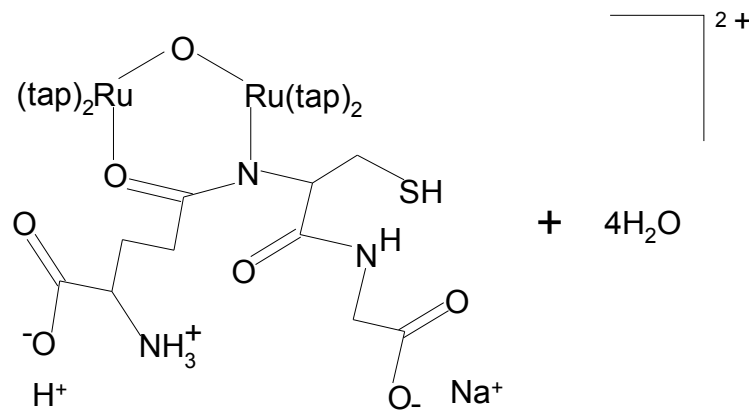


Fig. 9. ESI-MS spectra of GSH substituted product



m/z: 705.16

Effect of change in pH on the Reaction Rate

The reaction was studied at four different pH values. The k_{obs} values are found to increase with increase in pH in the studied pH range. The k_{obs} values are collected in Table 4.

Table 4. The $10^3 k_{1(obs)}$ and $10^5 k_{2(obs)}$ values at different pHs; $[1] = 1 \times 10^{-4} \text{ mol dm}^{-3}$, $[\text{Ligand}] = 3.0 \times 10^{-3} \text{ mol dm}^{-3}$, temperature = 50°C , ionic strength = $0.1 \text{ mol dm}^{-3} \text{ NaClO}_4$.

pH	$10^3 k_{1(obs)} (\text{s}^{-1})$	$10^5 k_{2(obs)} (\text{s}^{-1})$
5.5	0.46	1.55
6.0	0.55	6.6
6.5	0.58	3.0
7.0	2.16	3.33
7.4	2.65	7.8

The enhancement in rate may be explained based on two equilibria (equation 1 and equation 2). In the studied pH range (pH 5.5 to 7.4) with increase in pH the percentage of diaqua species is reduced and the percentage of the dimer is increased, and the dimer having two metal centers may be more acceptable to the incoming ligand. On the other hand with increase in pH the percentage of more reactive deprotonated ligand species increases which accounts for the increase in rate with increasing pH.

However, notwithstanding in the present kinetic runs (the effect of the variation of pH on rate), the substitution reaction was followed at pH 7.4, to avoid complications caused by adding an additional

parameter $[\text{H}^+]$ to the rate equation. We did not add any buffer in the kinetic solutions to maintain pH, because the buffer components may act as ligands. As during the reaction, no pH change was noticed (pH measured after the reaction was complete), the necessity of adding buffer was not important. Moreover, glutathione itself acts as a buffer.

Effect of Temperature on the Reaction Rate

The reaction was studied at four different temperatures for different ligand concentrations and the results are listed in Table 1 and Table 2. The activation parameters for the steps $1 \rightarrow \mathbf{B}$ and $\mathbf{B} \rightarrow \mathbf{2}$ are evaluated from the linear Eyring plots (Figure 9 and Figure 10) and

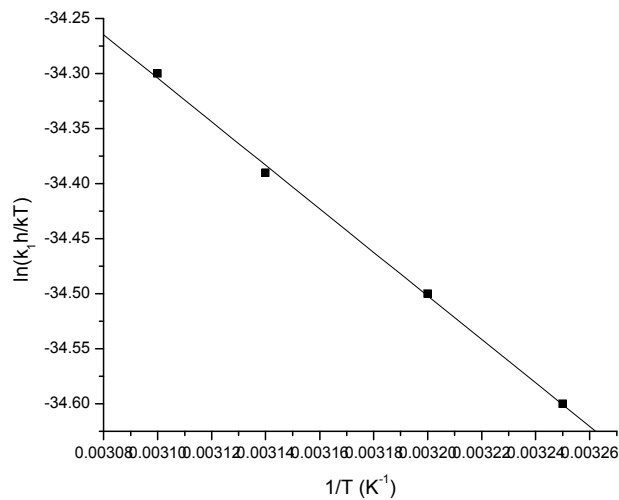


Figure 9. Eyring Plot ($\ln k_1 h/kT$ versus $1/T$) for the path 1.

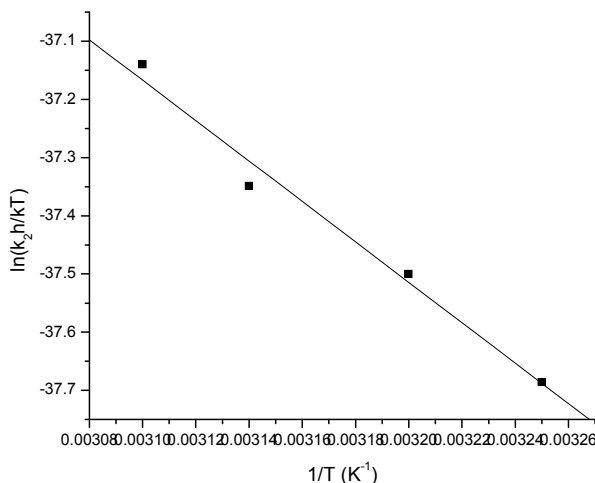


Figure 10. . Eyring Plot ($\ln(k_2 h/kT)$ versus $1/T$) for the path 2.

the results are compared with analogous systems (Table 5). The activation enthalpies and entropies are: $\Delta H_1^\ddagger = 16.4 \pm 4.2 \text{ kJ mol}^{-1}$, $\Delta S_1^\ddagger = -234 \pm 1 \text{ JK}^{-1} \text{ mol}^{-1}$, $\Delta H_2^\ddagger = 28.9 \pm 2.7 \text{ kJ mol}^{-1}$ and $\Delta S_2^\ddagger = -220 \pm 9 \text{ JK}^{-1} \text{ mol}^{-1}$. The low ΔH^\ddagger values are in support of the ligand participation in the transition state for both the steps. The positive energy required for the bond breaking process is partly

compensated from the negative energy obtained from bond formation in the transition state and hence a low value of ΔH^\ddagger is observed. The high negative ΔS^\ddagger values, on the other hand suggest a more compact transition state than starting complex and this is also in support of the assumption of a ligand participated transition state.

Table 5. Activation parameters for $[(H_2O)(tap)_2RuORu(tap)_2(H_2O)]^{2+}$ by various ligands in aqueous medium, $pH = 7.4$.

Ligand	ΔH_1^\ddagger (kJ mol ⁻¹)	ΔS_1^\ddagger (JK ⁻¹ mol ⁻¹)	ΔH_2^\ddagger (kJ mol ⁻¹)	ΔS_2^\ddagger (JK ⁻¹ mol ⁻¹)	Ref
Azide	14.1 ± 1	-240 ± 3	44.0 ± 1.5	-190 ± 4	19
Adenosine	9.0 ± 0.4	-266 ± 2	35.6 ± 2.2	-212 ± 7	19
Inosine	12.5 ± 1.1	-259 ± 3	28.9 ± 1.1	-230 ± 3	19
Uridine	12.5 ± 1.3	-255 ± 4	26.2 ± 2.9	-240 ± 9	19
Thioglycolic acid	10.6 ± 1.8	-262 ± 5	39.0 ± 2.4	-194 ± 7	19
Thiosemi-carbazide	14.2 ± 0.8	-241 ± 2	30.8 ± 1.4	-236 ± 4	19
Glutathione	16.4 ± 4.2	-234 ± 1	28.9 ± 2.7	-220 ± 9	this work

MECHANISM AND CONCLUSION

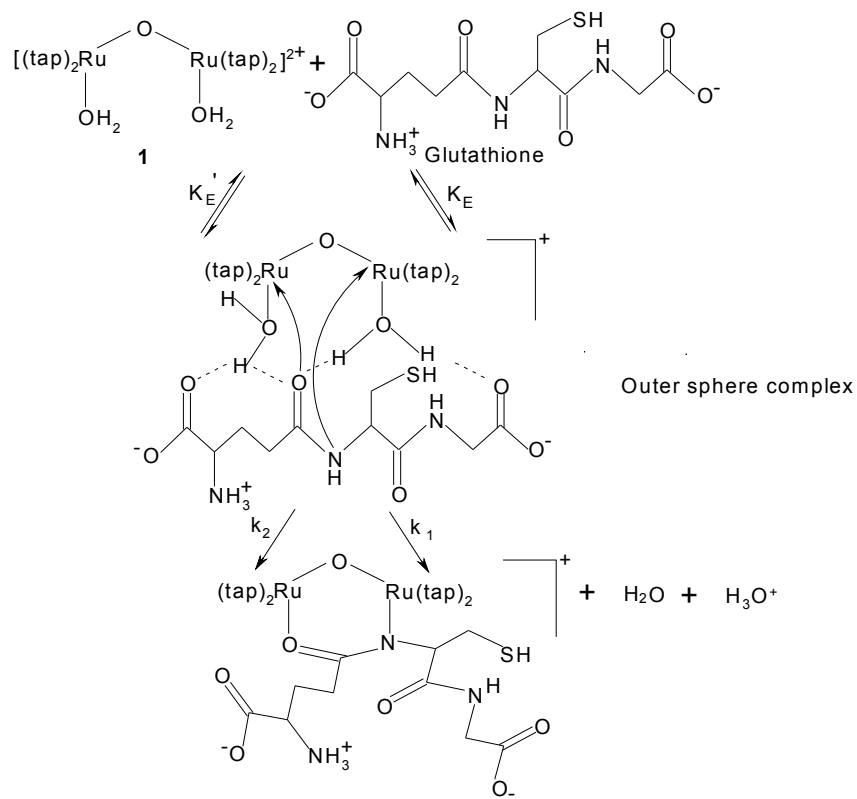
The bonding mode of GSH is not quite clear as repeated attempts to isolate the solid product were failed. Reduced glutathione (GSH) is a very versatile ligand, forming stable complexes with both hard and

soft metal ions. Several general binding modes of GSH are described. Soft metal ions coordinate exclusively or primarily through thiol sulfur. Hard ones prefer the amino acid-like moiety of the glutamic acid residue. Several transition metal ions

can additionally coordinate to the peptide nitrogen of the γ -Glu-Cys bond [38].

The interaction of glutathione with the title ruthenium complex proceeds *via* two distinct parallel paths of substitution of aqua molecules ($k_1 \sim 10^{-3} \text{ s}^{-1}$ and $k_2 \sim 10^{-5} \text{ s}^{-1}$). Glutathione with two different donor centers (N, O) attacks two borderline Ru(II) centers parallel, but with different reactivity. As the first step is $\sim 10^{-3} \text{ s}^{-1}$, which is much faster than the second step ($\sim 10^{-5} \text{ s}^{-1}$), thus when we are calculating this step the parallel contribution from the second step is negligible; and when we are calculating the second step, then the first step is already over. Thus although two steps are overlapping, there is no error in the calculation. Each path proceeds *via* an associative interchange mechanism. At the outset of each step an outer sphere complex results which is

stabilised through hydrogen bonding and is followed by an interchange from outer sphere to inner sphere complex. The outer sphere association equilibrium constants, a measure of the extent of hydrogen bonding for each path at different temperatures are evaluated (Table 3). From the temperature dependence of the K_E and K_E' the thermodynamic parameters are calculated: $\Delta H_1^\circ = 20.68 \pm 1.96 \text{ kJ mol}^{-1}$, $\Delta S_1^\circ = 105 \pm 6 \text{ JK}^{-1} \text{ mol}^{-1}$ and $\Delta H_2^\circ = 10.3 \pm 1.1 \text{ kJ mol}^{-1}$, $\Delta S_2^\circ = 66 \pm 4 \text{ JK}^{-1} \text{ mol}^{-1}$. ΔG° values, thus calculated for both the steps at all temperatures studied, have a negative magnitude which is once again in favour of the spontaneous formation of outer sphere association complex prior to the interchange of outer to inner sphere. A plausible mechanism may be shown in the following:



ACKNOWLEDGMENT

The authors acknowledge the University of Burdwan, Burdwan, West Bengal, India for extending all types of co-operation during this work.

REFERENCES

1. C. Orvig and M.J. Abram, *Chem. Review*, **99**, 2201 (1999).
2. Metals in Medicine, *J. Biol. Inorg. Chem.*, **12** (suppl 1), S7 (2007).
3. B. Rosenberg, L. Vancamp and T. Krigas, *Nature (London)*, **205**, 698 (1965).
4. *Cisplatin-chemistry and biochemistry of a leading anticancer drug*, (Eds.) B. Lippert, Wiley-VCH, Weinheim (1999).
5. R. V. Brabec, O. Novakova, DNA binding mode of ruthenium complexes and relationship to tumor cell toxicity, *Drug Resistance Updates*, **9**, 111 (2006).
6. I. Kostova, Ruthenium complexes as anticancer agents, *Cur. Med. Chem.*, **13**, 1085 (2006) and references therein.
7. J. Reedijk, *Pure and Appl. Chem.*, **59**, 181 (1987).
8. M. Zhao and M.J. Clarke M. J., *J. Biol. Chem.*, **4**, 325 (1999).
9. E. Galardon, P.Lc. Maux, A. Bondon and G. Simoncaux G., *Tetrahedron: Asymmetry*, **10**, 4203 (1999).
10. D.R. Frasca and M.J. Clarke, *J. Am. Chem. Soc.*, **121**, 8523 (1999).
11. V.G. Povsc, and J.A. Olabe, *Transition Met. Chem.*, **23**, 657 (1998).
12. M.J. Clarke, *Met. Ions Biol. Syst.*, **11**, 231 (1980).
13. R.E. Yasbin, C.R. Matthews and M.J. Clarke, *Chem. Biol. Interact.*, **31**, 355 (1980).
14. F. Legendre, V. Bas, J. Kozelka and J.C. Chottered, *Chemistry-A European Journal*, **6**, 2002 (2000).
15. P. Banerjee, *Coord. Chem. Rev.* **192**, 19. (1999).
16. M. Ray, S. Bhattacharya and P. Banerjee, *Indian J. Chem.*, **76A**, 151 (1999).
17. T. M. Buslavca & S. A. Simanova, *Russ. J. Coord. Chem.*, **25**, 151 (1999).
18. M. Shoukry & R. Van Eldik, *J. Chem. Soc., Dalton Trans.*, 2673 (1996).
19. A.K. Ghosh, *Transition Met. Chem.*, **35**, 885, (2010).
20. B.K. Ghosh and A. Chakraborty, *Coord. Chem. Rev.*, **95**, 239 (1989).
21. G. Wu, Y. -Z. Fang, S. Yang, J.R. Lupton and N.D. Turner, *J. Nutr.* **134**, 489 (2004).
22. D.A. Dickinson, D.R. Moellering, K.E. Iles, R.P. Patel, A.-L. Levonen, A. Wigley, V.M. Darley-Usmar, H.J. Forman, *Biol. Chem.*, **384**, 527 (2003).
23. S.C. Lu, *J. FASEB*, **13**, 1169 (1999).
24. P.M. Kidd, *Alt. Med. Rev.*, **1**, 155 (1997).
25. J. A. Weyh and R.E. Hamm, *Inorg. Chem.*, **8**, 2298 (1969).
26. B. Mahanti and G.S. De, *Transition Met. Chem.*, **17**, 23 (1992).
27. S.J. Raven and T.J. Meyer, *Inorg. Chem.*, **27**, 4478 (1998) and references cited therein.
28. W. Kutner, J.A. Gilbert, A. Tomaszewski, T.J. Meyer and R.W. Murry, *Electroanal. Chem.*, **205**, 185 (1986).
29. S.W. Gersten, J. Samuels and T.J. Meyer, *J. Am. Chem. Soc.*, **104**, 4029 (1982).
30. N. Bag, A. Pramanik, G.K. Lahiri, and A. Chakraborty, *Inorg. Chem.*, **31**, 40 (1992).
31. Z.D. Burgacic, G. Liehr and R.V. Eldik, *Dalton Trans.*, 2825 (2002)
32. D. L. Rabenstein, *J. Am. Chem. Soc.* **95**, 2797 (1973).
33. G.A. Jeffrey, *An Introduction to Hydrogen Bonding*, Oxford University Press, Oxford (1997).
34. G.R. Desiraju and T. Steiner T., *The Weak Hydrogen Bonding in Structural Chemistry and Biology*, Oxford University Press, Oxford (1999).
35. G. Pneumatikakis, and N. Hadjiliadis, *J. Inorg. Nucl. Chem.*, **41**, 429 (1979).
36. E. S. Raper, *Coord. Chem. Reviews.*, **61**, 115 (1985).
37. M. A. Taher, S. E. Jarelnabbi, B. E. Bayoumy, S. M. El-Medani, and R. M. Ramadan., *International Journal of Inorganic Chemistry*, doi:10.1155/2010/296215, 2010 (2010).
38. A. Krezel and W. Bal, *Acta Biochim Pol.* **46**, 567 (1999).